Transverse Shear Strength of Unidirectional Carbon Fiber Reinforced Aluminum Matrix Composite under Static and Dynamic Loadings

L. H. Dai and Y. L. Bai

Journal of Composite Materials 1998 32: 246
DOI: 10.1177/002199839803200303

Transverse Shear Strength of Unidirectional Carbon Fiber Reinforced Aluminum Matrix Composite Under Static and Dynamic Loadings

L.H. DAI* AND Y.L. BAI
LNM, Institute of Mechanics
Chinese Academy of Sciences
Beijing 100080, P.R. China

(Received November 15, 1996)
(Revised April 17, 1997)

ABSTRACT: The static and dynamic transverse shear strength of a unidirectional carbon fiber reinforced cast aluminum alloy matrix composite (C_f/A356.0) and aluminum alloy were studied with Instron-1195 testing machine and a split Hopkinson pressure bar, respectively. The results indicate that the transverse shear strength of the composite is about half that of the aluminum matrix. Both the composite and the matrix show almost the same rate effect, namely a slight increase in the shear strength with increasing strain rate. This may be an indication that the rate effect of the unidirectional C_f/A356.0 composite is mainly controlled by the A356.0 aluminum alloy matrix. Moreover, the shear failure mechanisms of the composite are discussed.

KEY WORDS: metal matrix composites, shear strength, high strain rate.

1. INTRODUCTION

THE FEASIBILITY OF using fiber reinforced composites for wide applications in engineering design in preference to conventional metallic materials has received considerable attention during the past few years. A dominant mechanical feature of the unidirectional fiber composites is their anisotropy, the longitudinal tensile strength being much greater than other tensile strengths and shear strength. An important consequence of this anisotropy is that an accurate evaluation of the shear strength becomes significant.

*Author to whom correspondence should be addressed. Present address: Department of Mechanics, Peking University, Beijing 100871, China.

0021-9983/98/03 0246–12 $10.00/0

In the last decade there have been several attempts to study shear response and fracture behavior of fiber reinforced polymer matrix composites (FRMMCs) at high strain rates by split Hopkinson bar technique with a variety of shear loadings and specimen geometries, Parry & Harding [1], Chiem & Liu [2] and Leber & Lifshitz [3]. A significant increase in shear strength with strain rates was observed with split Hopkinson torsional bars (SHTB) for both woven and cross-ply glass/epoxy composites. Moreover, there have also been attempts to use the split Hopkinson pressure bar (SHPB) for the study of shear strength of FRPMCs. Werner & Dharan [4] performed a test based upon short-beam shear of SHPB to investigate the interlaminar and transverse shear strength of a plain-wave carbon/epoxy laminates. The results showed no significant effect of strain rate. Bouetle et al [5] studied unidirectional carbon/epoxy composite with a double-notched specimen. Recently, Harding et al [6–7] suggested a double-lap and a single-lap shear specimen consecutively, to determine the shear strength of composite laminates.

Although a great progress has been made in the investigation of the dynamic shear strength of FRPMCs at high strain rates, very little attention has been paid to the ability of unidirectional fiber composites to resist to transverse shear failure and its rate effects. Furthermore, almost all studies were focused on FRPMCs. However, with increasing use of fiber reinforced metal matrix composites (FRMMCs) in engineering, to study the transverse shear strength of unidirectional FRMMCs and its rate effects become more and more important.

In this paper, the transverse shear strength of unidirectional C_f/A356.0 composite and A356.0 aluminum alloy under static and dynamic loadings were measured. The ability of unidirectional C_f/A356.0 composite to resist transverse shear failure and its rate effects were examined.

2. EXPERIMENTAL DETAIL

2.1 Materials

The unidirectional C_f /A356.0 composite and the A356.0 aluminum alloy were fabricated by the method of pressure infiltration casting under the same fabrication condition described as the following. The method and equipment used for pressure infiltration casting allow for inexpensive development and production of the composite materials. The set-up adopted in the present study is shown schematically in Figure 1. In brief, a block of A356.0 aluminum alloy was placed in a crucible and the pre-form of the unidirectionally aligned carbon fibers was then placed on the top of the block. The crucible was loaded into a furnace in a pressure chamber and melted under a vacuum. Aluminum liquid flowed around the pre-form, isolating the vacuum in the pre-form. Then the vessel was pressurized, forcing liquid into the pre-form. At last, the set-up cooled to the designed temperature (500°C) took the casting sample out. In our study, the casting sample is square bar with cross section 18 mm × 18mm. The

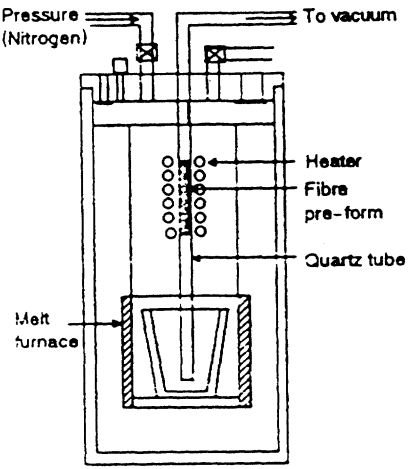

Figure 1. *Pressure infiltration casting set-up.*

fibers are aligned unidirectionally parallel to the central line of the bar, the fiber volume fraction is 50%. The microstructures of the unidirectional C_f /A356.0 composite are shown in Figure 2, which demonstrate that the carbon fibers are distributed uniformly and no obvious defects can be found in the interfaces between the fibers and the matrix. The nominal properties of the fiber and the matrix for the as-received composite are given in Table 1.

2.2 Specimen Geometry

Rectangular thin plate specimens, in which carbon fibers were uinidirectionally aligned in the direction parallel to the longer sides, were used in the present study. The specimens, with dimensions: L × B × H = 13 × 2 × 3 mm (Figure 3), were machined by the method of the electrical discharge cutting. In order to produce shear zones in the specimens, a stepped cylindrical head and a tubular support were used in the tests. The shape and dimensions of the head and the support are

Table 1. Nominal properties of fiber and matrix.

	Fiber	Matrix
Type	T-300	A356.0 aluminum alloy 7.0 Si-0.35 Mg-0.10 Ti
Diameter (μm)	7	—
Tensile strength (MPa)	3500	182
Tensile modulus (GPa)	235	80
Density (Mg/m^3)	1.76	2.72

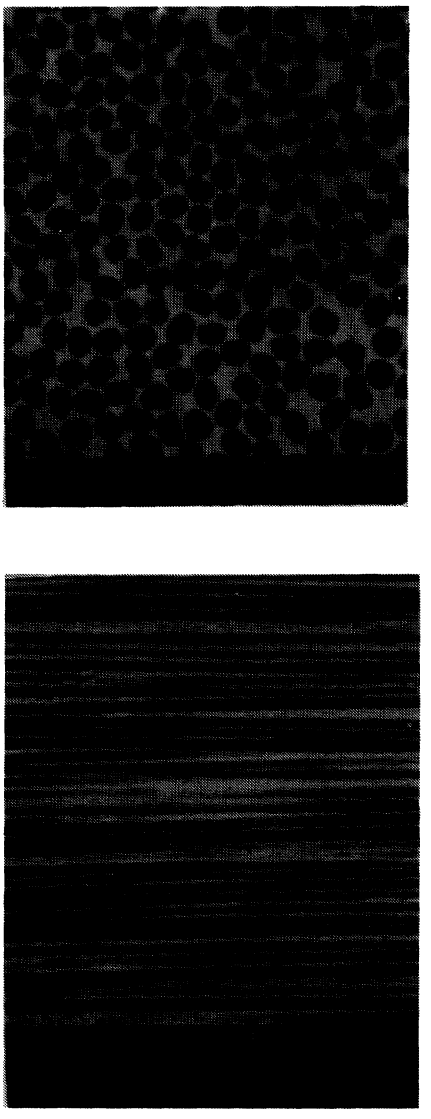

Figure 2. *SEM micrographs of C_f/A356.0 composite microstructure.*

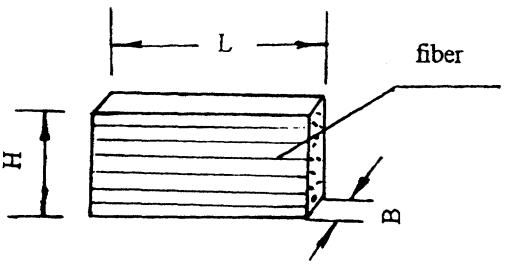

Figure 3. *Schematic description of the specimen and its dimensions.*

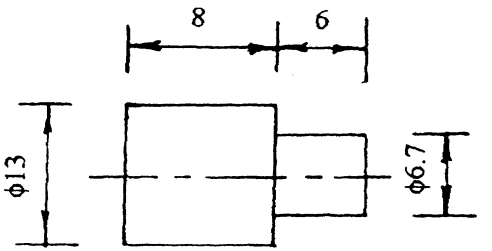

a) Head

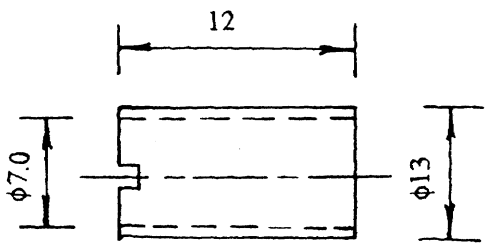

b) Support

Figure 4. *Schematic description of the impact head and the impact support.*

given in Figure 4. To avoid the deflection of the specimen, a notch,0.5 mm deep was cut on the support.

2.3 Static Tests

Static transverse shear tests were performed in an Instron testing machine. The cross head speed was of 2mm/min. The experimental arrangement is shown in Figure 5. In order to obtain accurate results , special attention was paid to the alignment of the head and the support during the testing. This is to make the two side clearances between the head and the support equal.

Because the width of the specimens is thin (~2 mm), the shear strength of the specimen can be calculated by

$$\tau_b = \frac{P_{max}}{2HB} \tag{1}$$

where P_{max} is the compression failure load, H and B are height and width of the specimen respectively (shown in Figure 3).

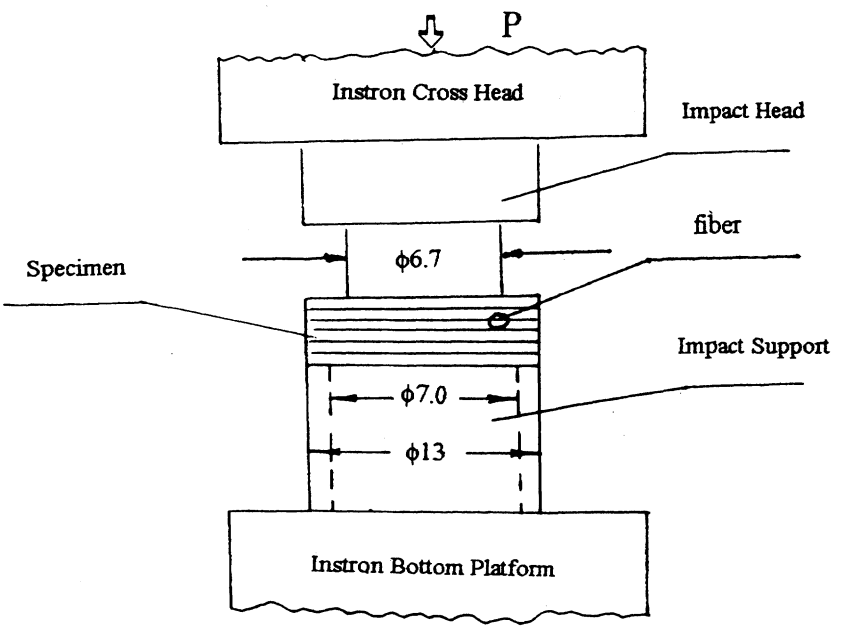

Figure 5. *Schematic description of static shear test system arrangement.*

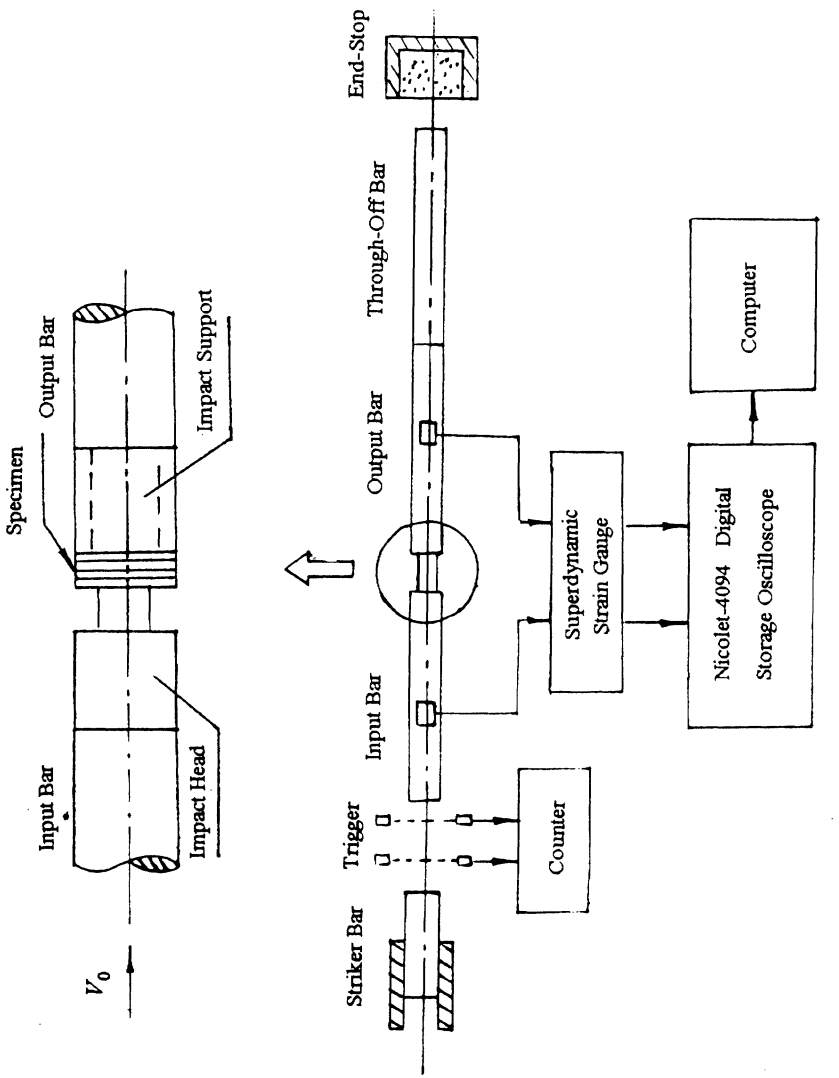

Figure 6. *Schematic diagram of the split Hopkinson bar apparatus and recording system.*

2.4 Dynamic Tests

Tests at high strain rates ($\sim 10^3$ /s) were performed with a modified split Hopkinson pressure bar apparatus, which is shown schematically in Figure 6. The pressure bars are made of high strength steel, 13 mm in diameter and 1m in length. A specimen was sandwiched between the stepped cylindrical head and the tubular support (shown in Figure 4). Then the whole assembly was sandwiched between the input and the output bars. An end-stop box at the end of the bar is used to absorb the residual axial momentum of the bars. The fibers in the specimen are unidirectionally aligned in the direction perpendicular to the loading direction.

The pressure pulse for each test was initiated by axial impact from the striker bar, which was accelerated to the desired impact velocity by compressed air. The striker bar, 0.3 m in length and 13 mm in diameter, is made of the same material as the pressure bars. This manner of loading produces a pressure pulse in the input bar with constant amplitude proportional to the impact velocity of the striker. Wave propagation effects in the specimen are ignored because the loading pulse is very long compared to the specimen length. To record the loading pulse, two pairs of strain gages were bonded at the mid span of the input and output bars respectively, which were parallel to the axis. In order to eliminate the bending wave effects and amplify the pulse signal, two strain gages in each pair were mounted on the opposite sides of the pressure bars and connected in series.

When the striker hits the input bar, a compressive pulse is produced, then propagates through the stepped cylindrical head, the specimen, the tubular support, and finally reaches the output bar. According the theory of one-dimensional elastic wave, the instantaneous stresses in the input and output bars can be expressed respectively as follows

$$\sigma_I = \rho_0 C_0^2 (\varepsilon_i + \varepsilon_r) \tag{2}$$

$$\sigma_T = \rho_0 C_0^2 \varepsilon_t \tag{3}$$

where ρ_0 and C_0 are the density and the longitudinal stress wave speed of the pressure bars, ε_i, ε_r and ε_t are incident, reflected and transmitted strain pulses respectively, which are recorded by the strain gages on both input and output bars.

In the light of the theory of one-dimensional elastic stress wave traveling through a bar with variational section, the stresses in the head and support are as follows

$$\sigma_I^0 = \frac{2A_0}{A_0 + A_I^0} \sigma_I \tag{4}$$

$$\sigma_T^0 = \frac{A_0 + A_T^0}{2A_T^0}\sigma_T \tag{5}$$

where A_0, A_I^0, and A_T^0 are the cross section areas of the pressure bars, the head and the support respectively.

According to the equality of the forces acted on the two sides of the specimen, one can derive [8]

$$\sigma_I^S = \frac{2A_0A_I^0}{(A_0 + A_I^0)A_S^I}\sigma_I \tag{6}$$

$$\sigma_T^S = \frac{A_0 + A_T^0}{2A_S^T}\sigma_T \tag{7}$$

where σ_I^S and A_S^I are the stress and the cross section area of the input side of the specimen (the side contacted with the head), while σ_T^S and A_S^T are the corresponding values of the output side of the specimen (the side contacted with the support).

Actually, shear takes place within the two thin layers of the thickness $(d_1-d)/2$ (shown in Figure 6), here d and d_1 are the diameter of the head and the inner diameter of the tubular support respectively. According to the force balance in the specimen, on the input side of the specimen,

$$\tau_1 \cdot 2HB = \sigma_I^S A_S^I \tag{8}$$

while on the output side of the specimen

$$\tau_2 \cdot 2HB = \sigma_T^S A_S^T \tag{9}$$

Substitution of Equations (6) and (7) into (8) and (9) respectively and the equality of the shear stress in the specimen: $\tau_1 = \tau_2 = \tau$, lead to the average shear stress in the specimen as follows

$$\tau = \frac{A_0A_I^0}{(A_0 + A_I^0)HB}\rho_0C_0^2(\varepsilon_i + \varepsilon_r) \tag{10}$$

or

$$\tau = \frac{A_0 + A_T^0}{4HB}\rho_0C_0^2\varepsilon_t \tag{11}$$

In our tests, the values calculated from Equations (10) and (11) are approximately equal, so Equation (11) was used to determine the shear strength.

3. RESULTS AND DISCUSSIONS

The static and dynamic transverse shear strength of both A356.0 aluminum alloy and unidirectional C_f/A356.0 composite are given in Table 2.

The most noticeable experimental result is that both the static and dynamic transverse shear strength of the C_f/A356.0 composite is much lower than that of the unreinforced matrix-A356.0 aluminum alloy. This implies that the unidirectionally aligned carbon fiber reinforced A356.0 composite is prone to transverse shear failure in our present experimental conditions.

It is well known that the failure of fiber reinforced composites usually results from nucleation and extension of internal microdamage. These are closely related to the micromechanical stress state of the composite. Some theoretical results demonstrate that the internal stress distribution of the unidirectional fiber composites subjected to a shear loading is nonuniform and very high stresses are concentrated on the interfaces [9–11]. Recently, more complete micromechanical stress analysis shows that very high stress concentrations exist in both interfaces and neighboring regions in the matrix for high density unidirectional fiber composites under shear loading [8]. This high stress concentration may induce interface debonding and matrix cracking before fiber fracture occurs. Microscopic observations of the fracture surfaces of the C_f/A356.0 composite both at static and impact loading with Scanning Electronic Microscope (SEM) verify the aftermentioned statement (Figure 7). In Figure 7, a vast amount of microdamage-interface debonding, cracks in matrix, and fiber pulled-out can be found. The nucleation, extension and coalescence of this microdamage, no doubt, deteriorate the ability of the fibers to bear loading and induces low transverse shear strength of the unidirectional C_f/A356.0 composite.

From the experimental results shown in Table 2, there is a slight strain rate effect on the shear strength of both A356.0 aluminum alloy and unidirectional C_f/A356.0 composite. The increments in the shear strength are 15 and 23 percent respectively. This is due to the difference of the plastic deformation in the matrix between the static and dynamic shearing cases [12]. Actually, from Figure 7 one can find the density of the cracks in the matrix on the dynamic shear failure surface of the composite is much lower than that on the static shear failure surface. In a dynamic case, the plastic flow was constrained owing to the very short duration of loading, which finally leads to higher shear strength than that of the static case. But the small difference of the strain rate effects between

Table 2. Transverse shear strength of A356.0 Al alloy and unidirectional C_f/A356.0 composite.

Materials	Static Shear Strength τ_b^s (MPa)	Dynamic Shear Strength τ_b^d (MPa)	$(\tau_b^d - \tau_b^s)/\tau_b^s$ (%)
A356.0 Al alloy	107 ± 2	123 ± 3	15
C_f/A356.0	52 ± 3	64 ± 5	23

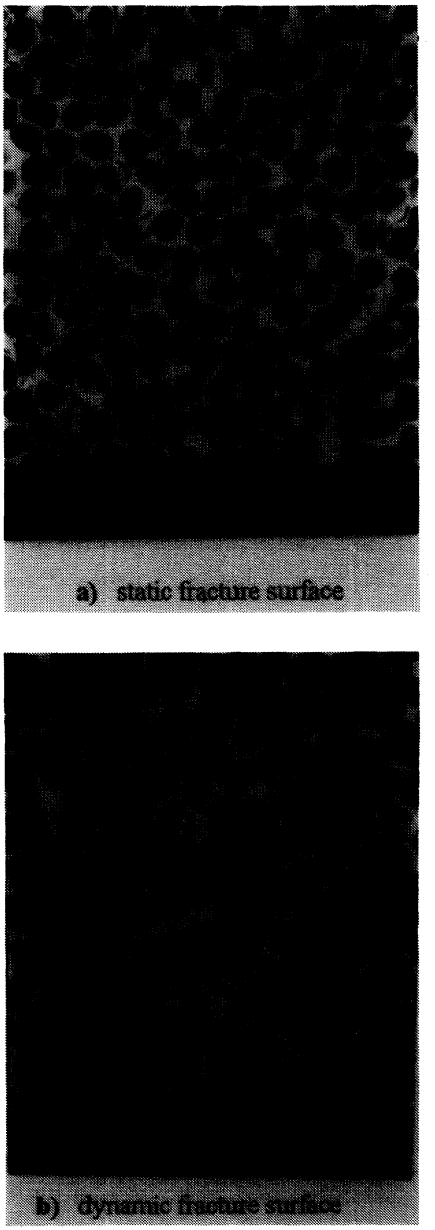

Figure 7. *SEM micrographs of fracture surfaces of* C_f */A356.0 composite.*

these two materials indicates that the strain rate effect of the unidirectional C_f /A356.0 composite is mainly controlled by the matrix. Theoretical results also support this point [13].

4. CONCLUSION

In conclusion, the static and dynamic transverse shear strength of both A356.0 aluminum alloy and unidirectional C_f/A356.0 composite were investigated by making use of an Instron testing machine and a modified split Hopkinson pressure bar. The results demonstrate that the transverse shear strength of the unidirectional C_f/A356.0 composite is much lower than that of the unreinforced matrix-A356.0 cast aluminum alloy. This is mainly due to the nucleation, extension and coalescence of the internal microdamage—interface debonding, cracks in the matrix etc., induced by the high stress concentrations in the interfaces and the matrix. This means that the unidirectionally aligned carbon fibers make no contribution to the ability of the unidirectional C_f /A356.0 composite to resist transverse shear failure. The results also show that the strain rate effect of the composite is mainly controlled by the matrix.

REFERENCES

1. Party, T. and J. Harding. 1981. Proc. of the colloque internal du CNRS. n°319.
2. Chiem, C.Y. and Z.Q. Liu. 1986. Proc. of the Internal. Symp. on Intense Dynamic Loading and Its Effects. Beijing. pp. 584–591.
3. Leber, H. and J.M. Lifshitz. 1996. *Comp. Sci. Technol.*, 56:391–405.
4. Werner, S.M. and C.K.H. Dharan. 1986. *J. Comp. Mater.* 20:365–374.
5. Boutile, B., C. Cazeneuve, & C. Oytana. 1992. *Comp. Sci. Technol.*, 45:313–321.
6. Harding, J. & Y.L. Li, 1992. *Comp. Sci. Technol.* 45:161–171.
7. Dond, L. and J. Harding. 1994. *Composites.* 25:129–138.
8. Dai, L.H. 1996. "Shear Failure Mechanisms and Strength Design of Fiber Reinforced Metal Matrix Composites." Thesis of Ph.D. Institute of Mechanics, Chinese Academy of Sciences.
9. Adams, D.F. and D.R. Doner. 1967. *J. Comp. Mater,* 1:4–17.
10. Goree, J.G. and H.B.Wilson. 1967. *J. App. Mech.* 34:511–515.
11. Budiansky, B. and G.F. Carrier. 1984. *J. App. Mech.* 51:733–735.
12. Bai,Y.L. & B. Dood, 1992. *Adiabatic Shear Localization-Occurrence, Theories and Applications.* Pergamon Press. Oxford, New York.
13. Dai, L.H. 1996. Proc. of ICAM. Bejing, pp. 986–990.